JKAU: Met., Env., Arid Land Agric. Sci., **vol. 9,** pp. 3-15 (1418 A.H. / 1998 A.D.)

Estimation of Minimum Land Surface Temperature Using the Special Sensor Microwave/Imager (SSM/I) over the Southwestern Region of Saudi Arabia

ABDUL-WAHAB S. MASHAT and AYMAN S. GHULAM
Faculty of Meteorology, Environment and Arid Land Agriculture
King Abdulaziz University, Jeddah, Saudi Arabia

ABSTRACT. The temperature of land surface over the southwest region of Saudi Arabia was inferred using passive microwave brightness temperatures sensed by the Special Sensor Microwave/Imager (SSM/I) on board a Defense Meteorological Satellite Program (DMSP). A linear regression analysis was used to correlate the SSM/I brightness temperatures or combinations of brightness temperatures with minimum screen air temperature (representing the minimum surface temperature) in a semi-arid, mountain region. Elevation correction and interpolation were performed. Two methods were used as "ground truth" for minimum air temperatures to investigate the response of SSM/I brightness temperatures to land surface temperatures (T1 and T2). It is shown that the brightness temperatures and the combination of brightness temperatures were poorly correlated with T1 and T2 where all data were used. Four methods were performed to determine the dry soil grid cells. Low correlation was found between brightness temperatures and combination of brightness temperatures and T1 and T2 over dry soil grid cells. Then the study area was divided into three regions: west, center, and east of the mountain. It is found that the brightness temperatures and combination of brightness temperatures were poorly correlated except that H37 channel showed the best channel response to T1 in the east region.

A single pixel linear correlation was performed on all the dry soil grid cells. It was found that H37 is the best single SSM/I channel to investigate land surface minimum temperature (T1) and H19 is the best single SSM/I channel to investigate land surface minimum temperature (T2).

Introduction

Passive microwave radiometery has provided good estimates of land surface temperatures (Lambert and McFarland, 1987; McFarland *et al.,* 1990; and Mashat and Alamodi, 1998). McFarland *et al*. (1990) used passive microwave brightness temperatures from the DMSP Special Sensor Microwave/Imager (SSM/I) to determine surface temperature over land areas in the central plains of the United States. A regression analysis

between all of the SSM/I channels and minimum screen air temperatures (representing the surface temperature) showed good correlations with root mean-square errors of 2.0-3.0°C. Mashat and Alamodi (1998) found that a good correlation coefficient occurred between the SSM/I brightness temperatures and land surface temperatures at satellite descending overpass time over Saudi Arabia. They showed that it was possible to estimate the average land temperature at about 6:00 p.m. local solar time using SSM/I brightness temperatures (V22, V37, H37, V85, H85) for areas of 1° latitude × 1° longitude grid. However, they found that poor correlation coefficients occurred between the SSM/I brightness temperatures and land surface temperatures at satellite ascending overpass time at about 6:00 a.m.. They explained that the low correlation is due to the differences in "ground truth" land surface temperature between eastern and western regions of Saudi Arabia at 6 o'clock in the morning.

The goal of this research is to identify the best channel or combination of channels from the Special Sensor Microwave/Imager (SSM/I) to estimate minimum land surface temperature over the southwestern region of Saudi Arabia. Statistical methods, such as regression of principal components and correlation analysis, are used in the examination. Linear regression equations will be presented, which yield an estimate of the land temperature. The accuracy of this estimate will be compared to the temperature variability found in the stations.

The Study Area

The area of study, southwestern region of Saudi Arabia, is bounded on the north by latitude 20° N, on the east by longitude 43° E, on the south by Yemen, and on the west by the Red Sea. The western coastal plain (known as Tihama) abuts the Red Sea. Its height gradually increases eastward to the foothills and then sharply to the Sarawat Mountains (Jubal Al-Sarawat), which are located 80 km parallel to the Red Sea from the east. These, in turn, are followed by the Najed Plateau and the Empty Quarter in the east. The mountains vary in width, reaching a maximum near the Yemen border, and rise to a height of approximately 3300 m near Al-Suda or Asir mountains. Many wadies drain on both sides of the mountains. These wadies are dry most of the time, except during flood occurrence. Wadies on the western side of the mountain draining toward Red Sea are characterizes by shorter channels and steep slope.

Data Collection and Preparation

Ground Truth Data

The daily minimum air temperature readings measured by synoptic stations are needed to provide a "ground truth" data. The regional data consist of daily values of minimum temperature, extracted from the records of the Meteorology and Environmental Protection Administration (MEPA), Ministry of Defense and Aviation, Jeddah, as well as data provided by the Hydrology Division, Ministry of Agriculture and Water, Kingdom of Saudi Arabia, Riyadh. Daily minimum air temperature data above the ground (measured at 1.5 m height) for nine stations (Table 1), located in the study area for the period July-September 1987, were selected.

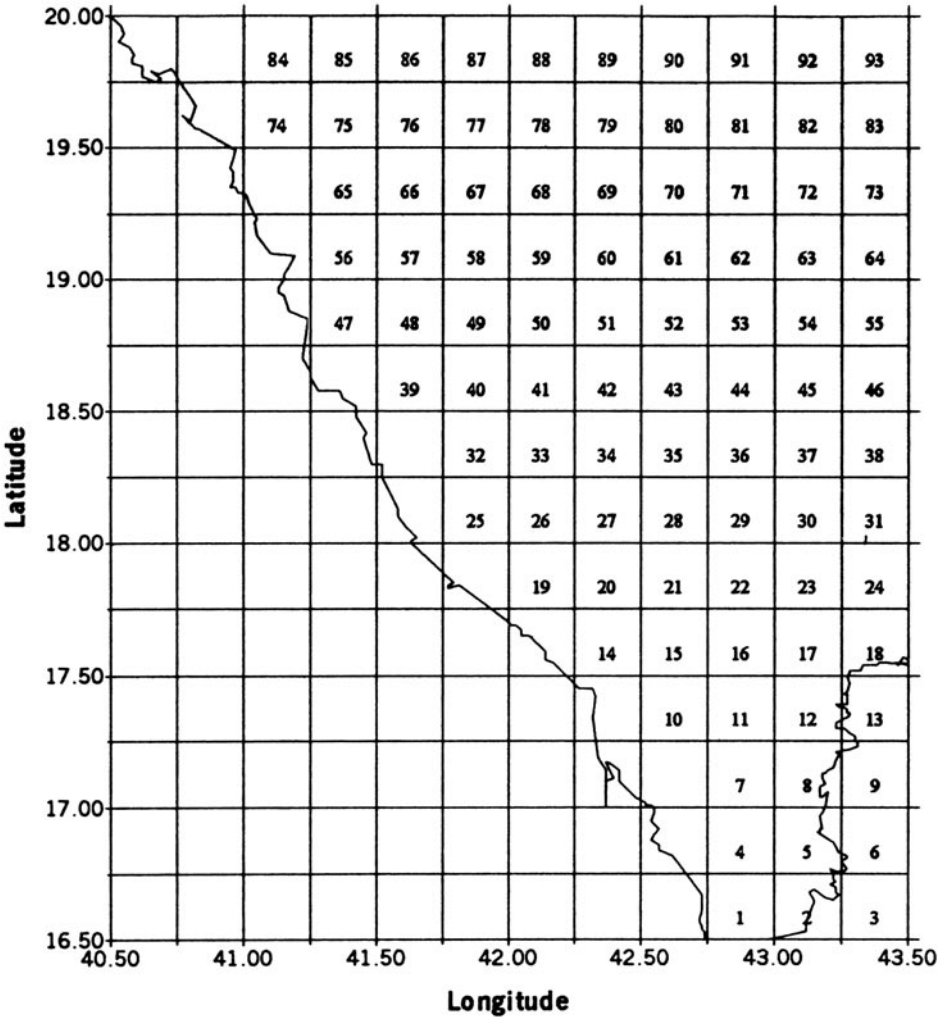

FIG. 1. Grid system of the study area (southwest of Saudi Arabia).

Because of the topographical difference in each grid cell, elevation corrections for temperatures are needed. In this study, regression analysis was carried out to correlate the monthly mean minimum temperature with stations elevations located in and near the area of study. The data used consisted of the records of 23 stations in or close to the study area, for each month (July - September, 1987). The analysis reveals that R^2 (the square of the linear correlation coefficient) is large ($R^2 = 0.841$). An equation relating the mean monthly minimum temperature, with elevation for the three months, was found as:

$$T_{elev} = -0.00579 \ *Z + 29.5009 \qquad \text{Eq. (1)}$$

TABLE 1. Available minimum temperature data for nine land stations in the study area.

Station name	Longitude (deg.)	Latitude (deg.)	Elevation (meter)
Kiyat	41.24	18.44	30
Biljurashy	41.33	19.52	2400
Abha	42.29	18.12	2200
Gizan	42.35	16.53	7
Sabya	42.37	17.10	40
Khamis	42.48	18.18	2056
Annimas	42.90	19.60	2600
Tathlith	43.31	19.32	975
Seratabida	43.60	18.10	2400

where T_{elev} is the temperature in °C at given elevation, and Z is the elevation in meter.

Because of the special resolution of the satellite images, the study area was divided into small grid cells ($0.25° \times 0.25°$). Grid cells that are the coastline were excluded from this study to avoid wet grid cells. It was found that ninety-three grid cells in the study area met the above conditions. The grid cells were numbered from the southwest beginning with number 1 and ending with number 93 (Fig. 1).

The elevation average for each grid cell for the study area was approximated using the topographic contour maps for the study area prepared by the Petroleum and Mineral Ministry, then a computer software program (SURFUR) was used to interpolate and distribute the mean elevation value at the center of each grid cell. To cancel topography effect, the minimum temperature for the nine stations (points) are plotted and then reduced (corrected) to mean sea level by two methods. The first method, used to reduce the minimum temperature to the mean sea level, was by using dry-adiabatic lapse rate (1°C/100 m). The second method to reduce the minimum temperature to the mean sea level, was by using Eq. (1). For both methods, isothermal lines are drawn manually (hand analysis) with an interpolation to define the aerial temperature average for each grid cell. Because the elevation for each grid cell was known, the minimum temperature for each grid cell was calculated by rising the temperature to the grid cell elevation by the above two methods. Two values of minimum land surface temperature were estimated; i) T1 by using the gradient of dry adiabatic lapse rate, and, ii) T2 by using Eq. (1). The estimated minimum temperature for each grid cell is assumed to represent the ground temperature at satellite ascending overpass time (about 6:00 a.m. local solar time).

The data used in this study contained Passive Microwave data from the Special Sensor Microwave/Imager (SSM/I). The calibrated brightness temperature data used in this study consisted of ascending passes for twelve days over the southwestern region of Saudi Arabia (Table 2). The means of brightness temperatures at each SSM/I frequency (19.35, 22.235, 37.0 and 85.5 GHz) were calculated for each grid cell consistent with "ground truth" in the form of a $0.25° \times 0.25°$ cell.

TABLE 2. The overpass SSM/I brightness temperature data over southwestern region of Saudi Arabia used for this study.

Date	Julian day	Revolution #
Jul 18, 87	199	396
Jul 25, 87	206	495
Aug 12, 87	224	749
Aug 13, 87	225	763
Aug 20, 87	232	862
Aug 21, 87	233	876
Sept 04, 87	247	1074
Sep 05, 87	248	1088
Sep 06, 87	249	1102
Sep 13, 87	256	1201
Sep 29, 87	272	1427
Sep 30, 87	273	1441

Analysis and Discussion

All Data Set

The initial data analysis consists of evaluating data set for all 93 grid cells using the satellite ascending overpass time (about 6:00 a.m. local solar time), for twelve days (1023 observations). Data set variables contained the grid cell number; Julian date; brightness temperatures (V19, H19, V22, V37, H37, V85, and H85, where V is the vertical polarization, H is horizontal polarization, and 19, 22, 37, and 85 are frequencies 19.350, 22.235, 37.000, and 85.500 GHz, respectively); ground minimum temperature (T1 and T2), calculated by two methods; polarization defference (Vf – Hf, where f is the frequency); polarization ratio (PRf, which is defined as [Vf – Hf] / [Vf + Hf]); and other algorithms.

Statistical analysis for brightness temperatures, land surface temperatures, polarization differences, and polarization ratios for all available SSM/I data, is shown in Table 3. For each channel, the vertically polarized brightness temperature is greater in value than the horizontally polarized brightness temperature. This agrees with the microwave physics in that the vertical polarization is greater than the horizontal polarization, and the difference increases with an increasing angle of incidence until Brewster's angle (about 70°) is reached (Mashat, 1992).

Using all data set (N = 1023), low correlation coefficients occur between the SSM/I brightness temperatures, combination of brightness temperatures, polarization difference, and polarization ratio with land surface temperatures. This is a result of differences in emissivity among the grid cells due to differences of many surface types (*i.e.* mountains, agriculture, and desert). The highest correlation coefficient (R = 0.4827), between T1 and brightness temperatures, was with V85. The highest correlation coefficient (R = 0.5437), between T2 and brightness temperatures, was with V85. The highest correlation coefficient, between T1 and combination of brightness temperatures, was with H19-H85 (R = – 0.5819). The highest correlation coefficient between T2 and

combination of brightness temperatures was with H19/H85 (R = – 0.6981), also, with H19-V37 (R = – 0.6948).

TABLE 3. Statistical analysis for brightness temperatures (ºK), land surface temperatures (ºK), polarization differences (ºK), and polarization ratios for all available SSM/I data for the period 18 July to 30 September, 1987 over southwestern Saudi Arabia.

Variable	Minimum	Maximum	Mean	Std. Dev.*	N+
V19	254.701	291.433	280.91	6.00	1023
H19	212.661	280.403	263.95	12.54	1023
V22	270.376	292.541	282.77	4.34	1023
V37	256.902	290.138	278.48	5.62	1023
H37	212.610	279.588	264.88	10.75	1023
V85	265.718	293.270	282.06	6.36	1023
H85	255.873	288.272	275.97	7.54	1023
V19 - H19	5.927	42.978	16.96	8.46	1023
V37 - H37	3.820	44.292	13.60	8.05	1023
V85 - H85	1.760	18.257	6.10	2.91	1023
PR19	.0106	.0908	.03	.02	1023
PR37	.0068	.2279	.03	.02	1023
PR85	.0031	.0335	.01	.01	1023
T1	280.000	312.600	296.51	6.50	1023
T2	282.220	306.542	294.59	5.42	1023

*Std. Dev. + Standard deviation, +N = number of observations.

Dry Soil Data Set

Many different methods were used in this study to define the dry soil grid cells and wet soil grid cells to avoid the effects of moisture. The dry soil grid cells data will be selected and analyzed, while the wet or moist soil grid cells will be excluded in this analysis. Mashat, (1992) found that the normalized brightness temperature in channel H37 with respect to land surface temperature (H37/T) was the best channel for surface soil moisture investigation at satellite ascending overpass time (6.00 a.m. local solar time). The formula was:

$$SM_{\frac{H\ 37}{T}} = 754.19\left(1 - 1.068\frac{H\ 37}{T}\right) \qquad \text{Eq. (2)}$$

where $SM_{\frac{H\ 37}{T}}$ is the soil moisture estimated using normalized brightness temperatures of H37.

Mashat and Sorman (1997) used algorithms denoted by the letters of [b], [d], [e], [g], and [m] to define dry and wet grid cells, where [b] = ((V19+V37)/2 - (H19+H37)/2), [d] = (V85-V37), [e] = (H85-H37), [g] = V19, and [m] = (H19-V85). Microwave band combinations [b], [d], [e], [g], and [m] together, distinguish dry areas from the wet areas in such a way that when soil in the ground surface is moist or wet, then [b] and [m] are expected to be less than 8.0 and (-6.0) respectively. On the other hand, when the values

of [b], [d], [e], and [m] get greater than 8.0, less than 1.0, less than 6.0, and less than (– 6.0) respectively, then the soil will be considered as dry soil (Mashat. and Sorman 1997).

To distinguish dry surface soil grid cells from the wet surface soil grid cells, four different methods were used. Eq. (2) was used twice ; once with T1 (method 1) and the other time with T2 (method 2) to define the dry soil surface grid cells. The third method (method 3), defines the dry soil surface grid cells under the condition of [b] ≥ 8.0 and [m] < 0.0. The fourth method (method 4) defines the dry soil surface grid cells under the condition of [b] ≥ 8.0, [d] < 1.0, [m] < – 6.0,and [e] < 6.0 (Mashat and Sorman, 1997).

The dry surface soil grid cells are selected, and the wet soil surface grid cells are excluded. The correlation coefficients of the land surface temperature T1 with brightness temperatures and combinations of brightness temperatures for dry soil surface grid cells using method 1 (N = 165) were calculated. Low correlation coefficients occur between the SSM/I brightness temperatures and combinations of brightness temperatures with land surface temperatures T1. The highest correlation coefficient between T1 and combinations of brightness temperatures occur with combinations H85/V85 and PR85 (R = 0.3974) for both combinations.

The correlation coefficients of the land surface temperatures T2 with brightness temperatures for dry soil surface grid cells using method 2 (N = 204) were also calculated. Low correlation coefficients occur between the SSM/I brightness temperatures and combinations of brightness temperatures with land surface temperature T2. The highest correlation coefficients between T2 and brightness temperatures occur with H85 (R = 0.6156), also, with V37 (R = 0.6006). The highest correlation coefficient between T2 and combinations of brightness temperatures occur with combination H85/V22 (R = 0.4955).

The correlation coefficients between brightness temperatures and land surface temperatures T1 and T2 for dry surface soil grid cells by using method 3 (N = 846) were calculated. The highest correlation coefficient (R = 0.5429) between T1 and brightness temperatures was with V85, while the highest correlation coefficient (R = 0.6020) between T2 and brightness temperatures was with V85. The highest correlation coefficient (R = 0.5939) between T1 and combination of brightness temperatures was with V37/V19, also with V19-V37 (R = -0.5931). The highest correlation coefficient between T2 and combination of brightness temperatures was with combination H19/H37 (R = 0.6999), also with combination H19/H85 (R =-0.6958). The correlation coefficients for T2 with brightness temperatures and combinations of brightness temperatures are higher than the correlation coefficients for T1 with brightness temperatures and combinations of brightness temperatures.

The correlation coefficients between land surface temperatures T1 and T2 and brightness temperatures and combinations of brightness temperatures for the dry soil surface grid cells using method 4 (N = 111 grid cells) were also calculated. Low correlation coefficients occur between the SSM/I brightness temperatures or the combinations of brightness temperatures and land surface temperature T1 or T2. The highest correlation co-

efficient (R = 0.2565) between T1 and brightness temperatures occur with V22. The highest correlation coefficient between T2 and brightness temperatures occur with V19 (R = 0.4006). The highest correlation coefficient (R = 0.2607) between T1 and combination of brightness temperatures occur with combination V19-V37. The highest correlation coefficient between T2 and combination of brightness temperatures occur with combination V19-V37 (R = 0.3329). The correlation coefficients of T2 with brightness temperatures and combinations of brightness temperatures are higher than the correlation coefficient between T1 and brightness temperatures and combination of brightness temperatures.

Western, Central, and Eastern Dry Soil Data

In the southwestern region of Saudi Arabia, the mountains (Asir mountains) vary in width, reaching a maximum near the Yemen border, and rise to a height of approximately 3300 m near Al-Suda. Minimum air temperatures for grid cells located at the top of the mountain are cold, due to topography. At the pass time of the satellite (6:00 a.m. local solar time), the sun has just risen, and the grid cells located to the east of the mountain have just begun to warm. On the other hand, the grid cells located to the west of the mountain are still under the shadow, and they are relatively cold. There is a contrast between the grid cells brightness temperatures due to their location in proximity (west or east) to the mountain, or at the top of the mountain (crest).

Using topographical map from Ministry of Petroleum and Minerals, the study area is divided into three regions, Central region (crest of the mountains), Western region (west side of the mountain), and Eastern region (east side of the mountain). The dry soil surface grid cells are selected to find correlation coefficients between T1, T2 and brightness temperatures and combinations of brightness temperatures for the three regions. The number of grid cells for each region for all surface categories are shown in Table 4.

TABLE 4. Number of grid cells for each region for all surface categories and for the dry land surface soil, for all area of the study and the three regions (West, Center, and East) after division.

Region	Number of grid cells (dry and moist soil)	Number of dry grid cells			
		method 1	method 2	method 3	method 4
All area of study	1023	165	204	847	111
West	484	075	097	432	005
Center (Crest)	110	064	079	041	003
East	429	026	028	374	103

Using method 1 to determine dry soil, the correlation coefficients between land surface temperature T1 and the brightness temperatures and combinations of brightness temperatures for each region are summarized as follow:

1) For the western region (N = 75), low correlations occur between land surface temperatures T1 and brightness temperatures and combinations of brightness temperatures. The highest correlation coefficient (R = 0.5509) occurs between T1 and brightness temperature H37.

2) For the central (crest) region (N = 64), low correlations occur between land surface temperatures T1 and brightness temperatures and combinations of brightness temperatures. The highest correlation coefficient (R = 0.4358) occurs between T1 and brightness temperature V37.

3) For the eastern region (N = 26), the highest correlation coefficient (R = 0.8680) occurs between T1 and brightness temperature H37.

Using method 2 to determine dry soil, the correlation coefficients between land surface temperature T2 and the brightness temperatures and combinations of brightness temperatures for each region are summarized as follow:

1) For western region (N = 97), the highest correlation coefficient (R = 0.5540) occurs between T2 and brightness temperature H85.

2) For the central (crest) region (N = 79), the highest correlation coefficient (R = 0.6637) occurs between T2 and brightness temperature V37.

3) For the eastern region (N = 28), the highest correlation coefficient (R = 0.7648) occurs between T2 and brightness temperature H19.

Using method 3 to determine dry soil, the correlation coefficients between land surface temperature T1 and T2 and the brightness temperatures and combinations of brightness temperatures for each region are summarized as follow:

1) For the western region (432 grid cells), the highest correlation coefficient between T1 and combinations of brightness temperatures occurs with combination V19-V37 (R = – 0.4733), also, with combination V37/V19 (R = – 0.4717). The highest correlation coefficient between T2 and combination of brightness temperatures occurs with combination V19-V37 (R = 0.6538), also, with combination V37/V19 (R = 0.6528).

2) For the central (crest) region (41 grid cells), the highest correlation coefficient (R = 0.5511) between T1 and brightness temperatures occurs with V85. The highest correlation coefficient (R = 0.6335) between T2 and brightness temperatures occurs with V85. The highest correlation coefficient between T1 and combination of brightness temperatures occurs with combination H37-V85 (R = – 0.5522). The highest correlation coefficient between T2 and combination of brightness temperatures occurs with combinations V85/V19 (R = 0.6154) and V19-V85 (R = – 0.654).

3) For the eastern region (374 grid cells), the highest correlation coefficient (R = 0.4048) between T1 and brightness temperatures occurs with H19. The highest correlation coefficients (R = 0.5645) between T2 and the brightness temperatures occurs with V19. The highest correlation coefficient between T1 and combinations of brightness temperatures occur with combination PR85 (R = -0.3846), also, with combination H85/V85 (R = 0.3833). The highest correlation coefficient (R = -0.4819) between T2 and combination of brightness temperatures occurs with combination H19-H85.

Finally, using method 4 to determine dry soil, the correlation coefficients between land surface temperature T1 and T2 and the brightness temperatures and combinations of brightness temperatures for each region are summarized as follow:

1) For the western region (N = 5), land surface temperature T1 was highly correlated with brightness temperatures, the highest correlation coefficient (R = 0.9758) occurs

with H85. Moreover, T1 was highly correlated with; V22 (R = 0.9755); V37 (R = 0.9748); H19 (R = 0.9697); H37 (R = 0.9647); V85 (R = 0.9647);and with V19 (R = 0.9644). The highest correlation coefficient (R = 0.9397) between T2 and brightness temperatures occurs with H85. Moreover, T2 was highly correlated with;V37 (R = 0.9138); V19 (R = 0.9260); V22 (R = 0.9055); and with V85 (R = 0.9035).

2) For central (crest) region (N = 3), the highest correlation coefficient (R = – 0.8571) between T1 and brightness temperatures occurs with H19. The highest correlation coefficient (R = – 0.9993) between T2 and brightness temperatures occur with V19. Moreover, T2 was highly correlated with; V22 (R = – 0.9888); V85 (R = – 0.9841); H85 (R = – 0.9761); H19 (R = – 0.9743); and with brightness temperature V37 (R = – 0.9348).

3) For eastern region (N = 111), low correlations occur between land surface temperatures T1 and T2 and brightness temperatures and combinations of brightness temperatures. The highest correlation coefficient (R = 0.4349) between T1 and brightness temperatures occurs with H19. The highest correlation coefficient (R = 0.4427) between T2 and brightness temperatures occurs with V19.

Case Study

To eliminate the effects of surface inhomogeneities, such as topographical differences and locations for the grid cells over the study area, each grid cell should be studied individually. Grid cell # 36 was selected as a case study grid cell. The Khamis-Mushait meteorological station is located at that grid cell. The correlation coefficients between T1, T2, station's temperature (ST) and SSM/I brightness temperatures were performed. It was found that T1 was highly correlated with the brightness temperature H37 (R = 0.8589), while T2 was highly correlated with brightness temperature H19 (R = 0.8321).

Conclusions

The major findings from this research are as given:

1. Poor correlation coefficients occurred between the SSM/I brightness temperatures and land surface temperatures for both T1 and T2 when all the grid cells were studied together.

2. Low correlation coefficients occurred between the SSM/I brightness temperatures and land surface temperatures T1 and T2 when all dry grid cell data set were used.

3. When the study area was divided into three regions (western, central, and eastern region), it was found that high correlation coefficients occurred between the SSM/I brightness temperatures and land surface temperatures T1 and T2.

4. By eliminating the influences among the grid cells, it was found that H37 is the best single SSM/I channel to use for a land surface minimum temperature T1 and H19 is the best single SSM/I channel to use for a land surface minimum temperature T2.

5. The SSM/I brightness temperatures can be used to classify near-land surface temperature over semi-arid mountain regions.

Recommendations

The outcome of this study indicates that the technology can be used to estimate near surface temperature, but additional studies are needed to evaluate other variables. It is

recommended that further studies needed to focus on the effects of surface inhomogeneities within the SSM/I footprints.

References

Lambert, V. M. and **McFarland, M.J.** (1987) Land surface temperature estimation over the northern Great Plains using dual polarized passive microwave data from the Nimbus 7. *Presented at the 1987 Summer Meeting ASAE Baltimore, MD, ASAE* Paper 87- 4041, 23 p.

Mashat, A. (1992) *Use of Special Sensor Microwave/ Imager (SSM/I) for Estimation of Precipitation Features in a Semi-Arid, Mountain Region: a Case Study of Southwest Saudi Arabia.* Ph. D. Dissertation, Texas A&M University, College Station, Texas.

Mashat, A. S. and **Alamodi, A.O.** (1998) Surface temperature estimation using Special Sensor Microwave/ Imager (SSM/I) data over Saudi Arabia. *J. KAU: Met., Env., Arid Land Agric. Sci.,* Vol. **8:** 15-26.

Mashat, A. and **Sorman, A.U.** (1997) Classification of the Surface Soil Moisture over a Semi-Arid Land Using the Special Sensor Microwave/Imager (SSM/I). *Civil Engineering Research Magazine, Al-Azhar University,* Cairo, Egypt. Vol. **19**(4): 476-491.

McFarland, M.J., Miller, R.L. and **Neal, C.M.U.** (1990) Land surface temperature derived from the SSM/I passive microwave brightness temperatures. *IEEE Trans., Geosci. Remote Sensing,* Vol. **28**(5): 839-845.

تقدير درجة الحرارة الصغرى لسطح الأرض باستخدام مجس حساس للموجات الدقيقة (SSM/I) فوق المنطقة الجنوبية العربية للمملكة العربية السعودية

عبد الوهاب سليمان مشاط و أيمن سالم غلام

قسم الأرصاد ، كلية الأرصاد والبيئة وزراعة المناطق الجافة

جامعة الملك عبد العزيز ، جـــــدة - المملكة العربية السعودية

المستخلص . تم القيام في هذا البحث بقياس ومقارنة درجات الحرارة الصغرى للمنطقة الجنوبية الغربية للمملكة العربية السعودية بواسطة القمر الصناعي SSM/I والذي يستخدم أشعة الميكروويف ، ودرجات الحرارة الصغرى المقاسة بواسطة محطات الأرصاد ، في نفس وقت مرور القمر الصناعي على منطقة الدراسة ، بهدف التوصل إلى قناة أو مجموعة من القنوات التي يستخدمها القمر ، لتمثل درجات الحرارة الصغرى في الأماكن غير المتوفر فيها محطات للرصد في منطقة الدراسة . ونظراً لاختلاف التضاريس في منطقة الدراسة ، فقد تم توزيع ارتفاعات بعض المحطات المتوفرة على كافة أجزاء المنطقة ، ولإيجاد العلاقة بين قراءات القمر الصناعي ومحطات الأرصاد ، تم حساب درجات حرارة المحطات المتوفرة في منطقة الدراسة على كافة الأجزاء باستخدام طريقتين لتوزيع درجات الحرارة ، وبهذا أصبحت لدينا قراءتين لدرجات الحرارة الصغرى في منطقة الدراسة (T1 و T2) .

أظهرت الدراسة أن درجات الحرارة المقاسة بكلا الطريقتين ترتبط ارتباطًا ضعيفًا مع تلك المقدرة بواسطة القمر الصناعي عند استخدام جميع المعلومات المتوفرة في منطقة الدراسة . وعليه فقد تم اختيار المربعات الجافة في منطقة الدراسة وذلك بأربع طرق مختلفة ، أظهرت الدراسة ارتباطًا ضعيفًا بين درجات الحرارة المقاسة بكلا الطريقتين وتلك المقدرة بواسطة القمر الصناعي . ومن ثم تم تقسيم المنطقة إلى أجزاء : غرب ووسط وشرق بناءً على تحديد المربعات التي تمر بها قمم الجبال ،

والتي تمثل وسط منطقة الدراسة ، والمربعات الواقعة غربها ممثل غرب منطقة الدراسة، أما المربعات الواقعة شرق قمم الجبال فتمثل شرق منطقة الدراسة ، فأظهرت هذه التقسيمات أن درجات الحرارة المقاسة بكلا الطريقتين ترتبط ارتباطًا ضعيفًا ماعدا درجة الحرارة (T1) والتي ترتبط مع الموجة H37 (تردد أفقي ٣٧ جيجاهيرتز) للقمر الصناعي ارتباطًا عاليًا . ولإيجاد علاقة أفضل فقد تم اختيار مربع واحد يحتوي على محطة رصد وذلك لمقارنة درجة الحرارة المقاسة بكلا الطريقتين مع قراءة القمر الصناعي وقراءة المحطة نفسها ، وقد أظهرت الدراسة أن أفضل موجة للقمر الصناعي نستطيع اعتبارها ممثل درجة الحرارة (T1) هي H37 بينما أفضل موجة للقمر الصناعي تمثل (T2) هي الموجة H19 (تردد أفقي ١٩ جيجاهيرتز) .